0273-2289/98/70–72—0615$11.25

Improved Oxygen Delivery in a Continuous-Roller-Bottle Reactor

R. Eric Berson, Trupti V. Mane, C. Kurt Svihla, and Thomas R. Hanley*

Department of Chemical Engineering, University of Louisville, Louisville, Kentucky 40292

ABSTRACT

Variations to the original aeration system in a continuous roller bottle reactor of novel design have been tested and compared for optimal oxygen (O) delivery. Reactor operating parameters that affect O transfer are rotation rate, liquid-volume level, fresh-feed rate, and supplementary-aeration rate. Design modifications to enhance gas–liquid O transfer include the addition of wall baffles and center baffles. The number and location of each of these baffles are compared for their effect on k_La values in the reaction chamber. The liquid feed into the system has been modified to improve the axial liquid mixing and O transfer.

Index Entries: Roller bottle reactor; continuous reactor; gas–liquid mixing.

INTRODUCTION

The capability of a cell culture to propagate can be limited if adequate oxygen (O) is not supplied efficiently throughout the system. Therefore, it is important to control the aeration and agitation system to prevent O from becoming a growth-limiting factor. Live plant or animal cells in culture are easily damaged, though, as a result of hydrodynamic stress caused by the aeration and/or agitation system used for supplying O. Hybridomas are reported to be sensitive to shear stresses beyond 1–5 N/m^2 *(1–3)*. Both O supply and hydrodynamic stress need to be considered when operating a bioreactor with cultures at high density.

Conventional roller bottles are used to grow plant or animal cells that may be too fragile to survive in the high-shear environment prevailing in conventional reactors used for submerged culture. The roller bottle may also be advantageous for growing attachment-dependent cells, since it can

* Author to whom all correspondence and reprint requests should be addressed.

provide a suitable solid surface for attachment. Conventional roller bottles are operated in batch: That is, they are filled initially with media and inoculated, and are then harvested after some set period of operation. The continuous-perfusion roller bottle reactor is designed to provide for the continuous supply of nutrients in a novel, mechanically simple manner. Continuous supply of medium, coupled with continuous or intermittent cell or product harvest, should result in a longer production phase, and in more efficient use of cells and medium. Media costs in cell culture can be extraordinarily high, and any means by which production can be extended, or media usage decreased, has the potential to offer large economic benefits.

The continuous-perfusion roller bottle reactor has already been used in the production of taxol from *Taxus* nodule culture, production of microtubers using *Solanum tuberosum*, and the growth of human carcinoma (HeLa) cells. These encouraging initial results have led to planned applications, including the production of rotavirus using epithelial cell lines, the production of differentiated colon carcinoma cells, the growth of *Francisella tularensis* (an intracellular bacterial pathogen), and other industrially important bioprocesses. One factor that has unlimited potential for development of new applications is the novelty of the design, which presents several features not found in conventional roller bottle reactors. The advantages offered by the continuous roller bottle design are primarily those that involve the supply of O and liquid nutrients to the cells. This work has therefore concentrated on establishing baseline data and quantitative models for the performance of the continuous roller bottle reactor from an engineering viewpoint, including the transfer of O from gas to liquid phase, and the supply and dispersion of liquid nutrients throughout the reaction chamber.

METHODS

Figure 1 shows the flow diagram for the various streams in the continuous perfusion roller bottle design. Salient features include the rotating drum wrapped with tubing (or spiroid), which pumps gas and liquid continuously from the fresh medium chamber to the reactor chamber; the sample loop spiroid, which provides a mean of monitoring the vessel contents, as well as enhancing the axial mixing and gas–liquid oxygen transfer in the chamber; and the outlet chamber, for harvesting product and cells. The sample loop spiroid picks up alternating plugs of gas and liquid (as it repeatedly passes through the liquid, then the headspace) from the near end of the vessel chamber, and pumps it through the external piping of the sample loop and the long pipe running through the center of the reactor, before depositing it at the far end of the chamber. The use of rotating spiroids to pump gas and liquid is mechanically simple, because the reactor needs only one moving part to turn both the reaction chamber and both

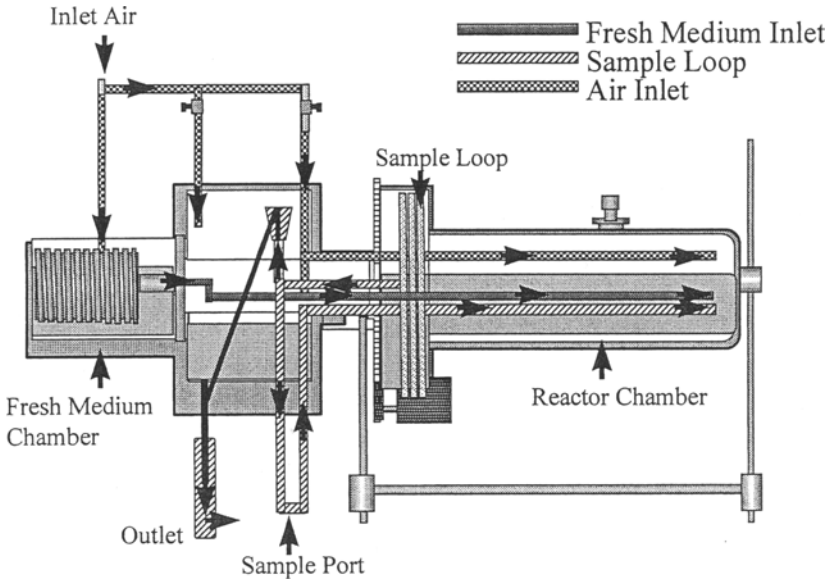

Fig. 1. Flow diagram of continuous roller bottle reactor.

spiroids. As the cells are pumped through the sample loop spiroid, low shear forces are maintained, which should pose no danger to fragile cell walls. The fresh medium chamber spiroid does deliver both gas and liquid to the cells in the reactor chamber, but supplemental gas can be introduced if O demand or removal of product gas requires higher gas throughputs than the spiroid can deliver. As shown in Fig. 1, the sample loop spiroid picks up gas and liquid from the near end of the vessel chamber and pumps it through the external piping of the sample loop and the long pipe running through the center of the reactor, before depositing it at the far end of the chamber. This loop provides a means for sampling the vessel contents, and, in addition, enhances the axial circulation of fluid in the vessel chamber.

The roller bottle chamber has a length of 0.610 m, a diameter of 0.0914 m, and a full-scale capacity of 4 L. Tests were conducted, using tap water and a liquid volume of 1.0 L, at nominal rotation rates of 2.0, 4.0, and 8.0 rpm. Each baffle has a length of 0.584 m and a width of 0.0254 m. If tests were taken with two baffles, the baffles were installed with 180-degree spacing. If three baffles were used, the baffles were installed with 120-degree spacing.

Modeling and Measuring Axial Dispersion in the Roller Bottle Reactor

These initial studies are concerned primarily with dispersion of the reactor feed, including nutrients from the feed inlet port, or the distribution

of O–enriched liquid from the sample recirculation loop. Since complete dispersion is typically achieved within about 2–3 residence times (based on the recirculation loop flow rate), the inlet and outlet flows can be neglected. The recirculation flow rate is over 10× the input and output flows at the highest rotational speed. The tests are conducted by injecting a 5–10-mL pulse of fluid containing indigo disulfonate tracer (approx 5×10^{-3} *M*) into the sample loop at the point where the loop re-enters the reactor. Samples are taken by syringe from the same port where the sample was introduced, with sampling continued until there is no appreciable variation in the tracer concentration. Tracer concentration is detected by absorbance at 610 nm using a UV/VIS spectrophotometer. The absorbance readings are normalized by dividing by the absorbance reading after the tracer has become uniformly dispersed.

If the level in the reactor is below that of the central tube assembly, the inlet liquid sometimes drips onto the liquid surface over a distance of a few centimeters. To treat this sort of initial dispersion, the following approach was developed. The region at the far end of the reactor chamber is assumed to consist of a well-mixed zone, into which the inlet pulse of tracer is uniformly dispersed. The size of this region is estimated by visually observing the tracer introduction for each test. The rest of the reactor is assumed to be described by a dispersion model. When developing the differential equation describing the well-mixed entry region, it is important to include the term for dispersion at the edge of the boundary with the dispersion region. The boundary conditions for the dispersion region then consist of the appropriate terms for the well-mixed zone at the entry end, and a zero gradient condition at the far end of the reactor, where the sample loop pick-up is located. Flow enters the well-mixed region from the sample loop return line at a rate given by the measured recirculation loop flow rate. The initial conditions for the simulation are specified by assuming that the tracer starts by being uniformly dispersed in the well-mixed entry region, with zero initial concentration throughout the dispersion region.

Well-Mixed Entry Region:

$$dC_E/dt = F/V_E\,(C_L - C_E) + D_eA/V_E\,dC/dz|_{z = L_1} \tag{1}$$

Initial condition:

$$C_E(t = 0) = C_{E0} \tag{2}$$

Dispersion Region:

$$\partial C/\partial t = D_e\,\partial^2 C/\partial z^2 - u\,\partial C/\partial z \tag{3}$$

Boundary conditions:

$$\text{At } z = L_1: \quad C(t, L_1) = C_E \tag{4}$$

$$\text{At } z = L: \quad \partial C/\partial z = 0 \tag{5}$$

Initial condition:

$$C(0, z) = 0 \tag{6}$$

Eq. 3 is solved using a finite difference approach with N equally spaced points. The resulting set of N ordinary differential equations is solved using the IMSL routine DIVPAG, which uses Gear's method, since initial value problems of this type tend to be stiff. The amount of tracer specified in the simulation is adjusted, so that the final concentration is 1. This technique provides a convenient basis for a dimensionless concentration, and allows the validity of the converged solution to be easily checked. In preliminary simulations, the number of points used in the simulation was set to 400, for which acceptable accuracy was achieved within a reasonable computation time. A typical result of the axial dispersion modeling is shown in Fig. 2, which shows both the experimental and simulated tracer response curves for a given set of conditions.

The reactor was modified to allow for multiple liquid inlet locations, as shown in Fig. 3. The modification was made to enhance axial liquid dispersion. Tests to measure the dispersion coefficient were conducted for one, two, and three wall baffles, using this modification.

Modeling Gas–Liquid Oxygen Transfer in the Roller Bottle Reactor

The sample loop increases the rate of O transfer to the liquid in the chamber, and, as a consequence, creates an axial gradient of dissolved O concentration in the vessel chamber. Therefore, in order to analyze tests conducted with the sample loop in operation, it is necessary to account for the presence of the axial concentration gradient, as well as the additional O transfer that takes place in the sample loop. The dispersion model presented to model the dispersion of a liquid-phase tracer can easily be adapted for this purpose. In the modified model, terms to account for the transfer of O from gas to liquid phase are simply added to the differential equations describing the entry region and the dispersion region. The balance on the well-mixed entry region is also modified by changing the concentration of the incoming liquid from the sample loop from C_L to C_{IN}, to reflect the additional O transfer that occurs within the sample loop. Previously, flow through the sample loop had been treated simply as a dynamic lag, which had been neglected, based on the relative time-scales of the tracer test and flow through the loop. A mass balance is then written to account for O transfer within the sample loop itself, based on the assumption that flow through the loop takes place in plug flow. The modified form of the model, which incorporates gas–liquid O transfer, is shown below.

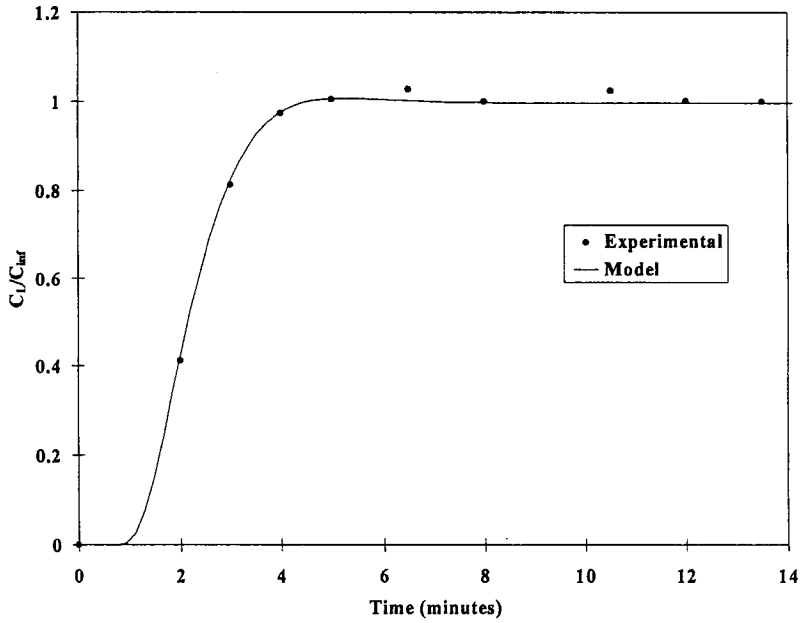

Fig. 2. Fit of dispersion model to experimental data (2 wall baffles, V = 1.0 L, 8 rpm).

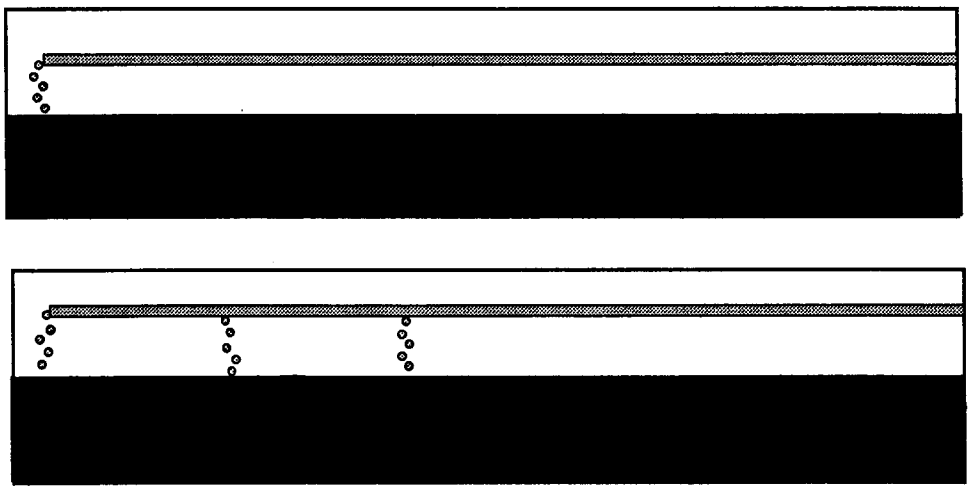

Fig. 3. Modified liquid return location.

Well-Mixed Entry Region

$$dC_E/dt = F/V_E\,(C_{IN} - C_E) + D_eA/V_E\,dC/dz|_{z = L_1} + k_La\,(\alpha C_G - C_E) \quad (7)$$

Initial condition:

$$C_E\,(t = 0) = C_{E0} \quad (8)$$

Dispersion Region:

$$\partial C/\partial t = D_e\,\partial^2 C/\partial z^2 - u\,\partial C/\partial z + k_La\,(\alpha C_G - C) \quad (9)$$

Boundary conditions:

$$\text{At } z = L_1\text{: } C(t, L_1) = C_E \quad (10)$$

$$\text{At } z = L\text{: } \partial C/\partial z = 0 \quad (11)$$

Initial condition:

$$C(0, z) = 0 \quad (12)$$

Sample Loop Region:

$$C_{IN} = \alpha C_G - (\alpha C_G - C_L)e^{-(k_La)_{SL}t_R} \quad (13)$$

Since the value of αC_G can be determined by noting the value of C_∞ and the residence time of fluid in the sample loop, t_R can determined by visual observation, the only two adjustable parameters in the model are the volumetric mass-transfer coefficients in the vessel and in the sample loop (k_L a and $(k_L\ a)_{SL}$, respectively). Dissolved O concentration can be measured both in the sample loop and within the vessel, in order to facilitate the determination of the two different dynamic terms. The partial differential equations describing the simultaneous processes of axial dispersion and gas–liquid mass transfer are solved using the same approach used for the analysis of liquid mixing.

Measurement of Gas–Liquid Mass-Transfer Coefficients

Tests were initially conducted in batch, with the sample loop inlet and exit ports capped. The axial concentration profiles modeled using the dispersion equation exist only when the sample loop is functioning; therefore, analysis of the experimental data is simplified considerably when the sample loop is disabled. The balance reduces to:

$$\partial C/\partial t = k_La\,(\alpha C_G - C) \quad (14)$$

Volumetric gas–liquid mass-transfer coefficients, k_La, were measured

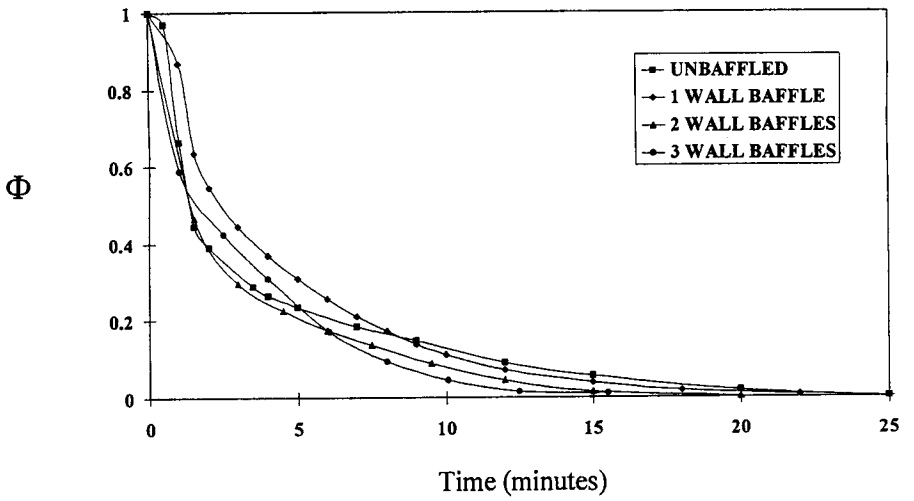

Fig. 4. Dissolved oxygen response curves (V = 1.0 L, 8 rpm).

using a dynamic technique. With the vessel held stationary, the gas headspace was sparged with O. Rotation at the desired rate was then initiated, and the resulting dissolved O response monitored until a new steady state was reached. A dissolved O electrode was inserted into the reactor chamber through the vessel inoculation port and periodically monitored until the liquid phase reached saturation. The data were fitted to a first-order response, with the time-constant from the fit taken as $1/k_La$. R^2 values ranged from 0.906 to 0.995. The k_La values obtained in the dynamic tests are nearly linear with rotation rate, which is consistent with data reported for unbaffled horizontal rotating vessels *(4,5)*.

Further tests were conducted with baffles installed either at the wall or in the center of the tank. Center baffles were attached to the gas and liquid inlet rods running through the center of the reaction chamber. Tests were conducted with one, two, or three baffles, and compared for k_La and effective dispersion coefficient, D_e, values.

In order to assess the significance of the O transfer in the sample loop to the overall rate of supply to the chamber, tests were also conducted with the sample loop in operation. The tests were conducted as described previously, except that the O electrode was inserted into the external piping of the sample loop, and monitored until the reading reached saturation.

RESULTS

Figure 4 shows the dissolved O response as a function of time for three wall baffle conditions. Initial concentrations are normalized at a value of 1 with no O yet transferred from the gas to the liquid. As the normalized concentration approaches zero, the concentration of O in the liquid phase

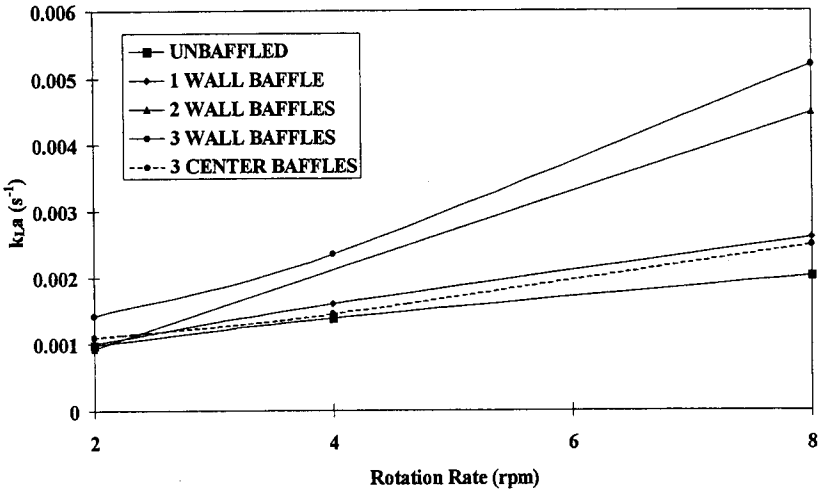

Fig. 5. Effect of baffles on k_La in the chamber (V = 1.0 L).

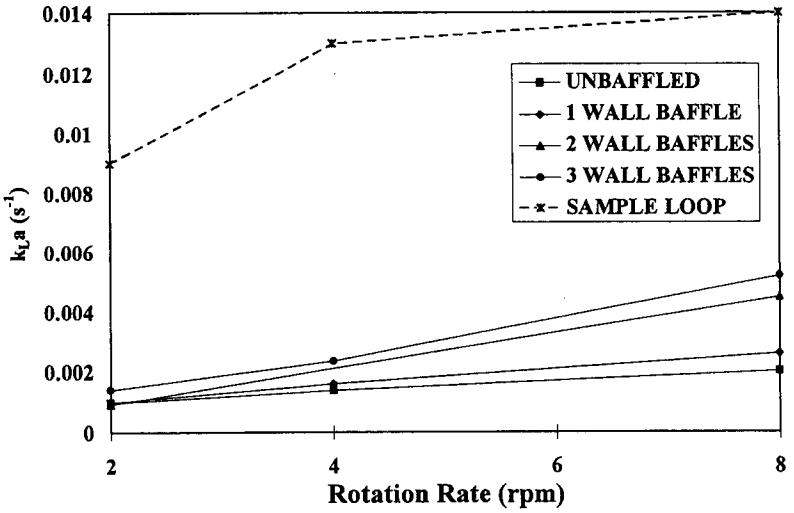

Fig. 6. Comparison of k_La in chamber and sampling loop (V = 1.0 L).

approaches equilibrium. As the number of baffles increase, the O concentration in the liquid reaches saturation more quickly.

Figure 5 shows how the number of baffles affects k_La. As the number of wall baffles increase, k_La increases. The effect is more pronounced at higher rotation rates. The results also indicate that wall baffles are more effective than center baffles. Three center baffles resulted in a lower k_La than a single wall baffle, for the rotation rates studied.

Figure 6 shows k_La values in the sampling loop. Note the enhancement of O transfer here, compared to in the reaction chamber.

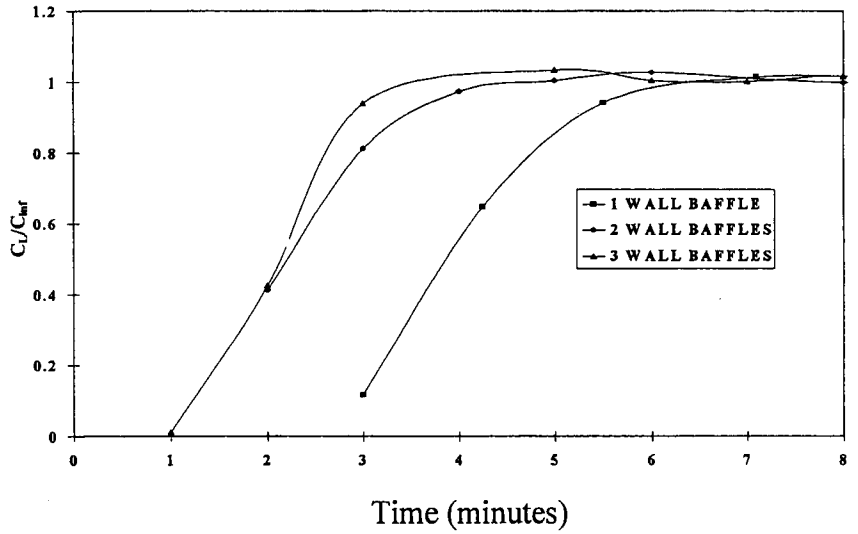

Fig. 7. Effect of baffles on tracer dispersion in the chamber (V = 1.0 L, 8 rpm).

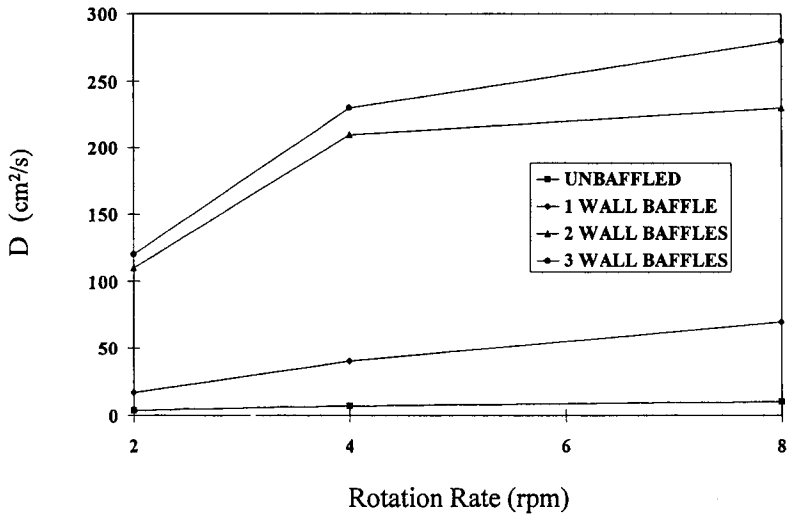

Fig. 8. Effect of wall baffles on liquid dispersion in the chamber (V = 1.0 L).

Figure 7 shows the effect of baffles on tracer dispersion in the reaction chamber. Tracer concentration is normalized by dividing by final tracer concentration. Increasing the number of wall baffles results in a quicker rise to equilibrium concentration.

Figure 8 shows the effect of the addition of wall baffles on liquid dispersion. Increasing the number of wall baffles results in higher values of D_e.

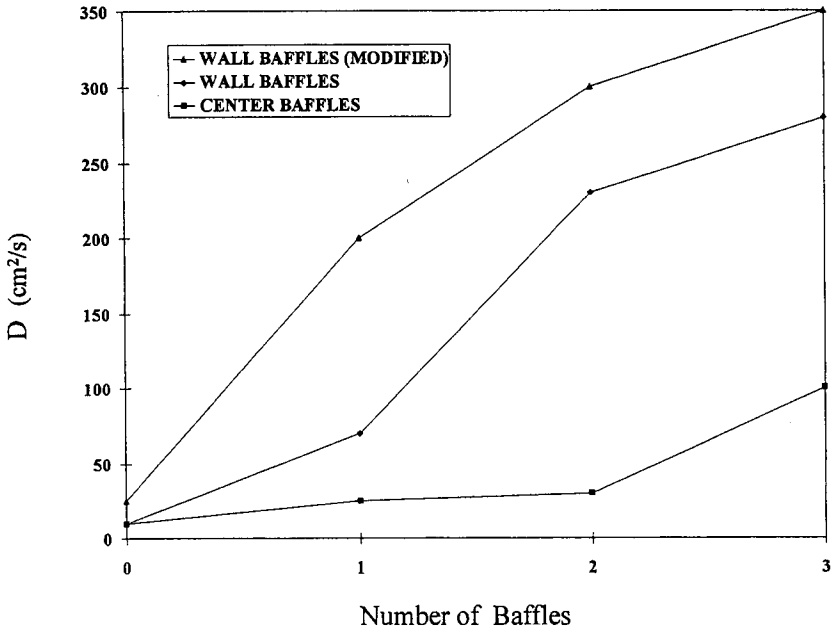

Fig. 9. Effect of baffle location and reactor modification on liquid dispersion (V = 1.0 L, 8 rpm).

Figure 9 compares D_e values for various reactor configurations. Results for center baffles, wall baffles, and wall baffles with modified liquid return inlet locations are shown. The tests with the modified liquid return inlet locations resulted in the greatest values of D_e.

DISCUSSION

The sampling loop provides a means for sampling the vessel contents, and, in addition, enhances the axial circulation of fluid in the vessel chamber. As the gas and liquid flow through the turns of the spiroid and the piping of the sample loop, the two phases are brought into close and vigorous contact. This contact results in a relatively high value of k_La. The concentration of dissolved O in the liquid phase flowing through the sample loop increases substantially over the prevailing value in the reactor. Thus, in terms of monitoring the dissolved O concentration in a dynamic test, the sampling loop is not truly a sampling loop, since its dissolved concentration is greater than the average value in the reactor. The sampling loop also represents a region of enhanced gas–liquid O transfer that is not present in a conventional roller bottle.

Although k_La in the sampling loop can be 9× the k_La in the chamber, the residence time in the loop is much smaller than the residence time in the chamber. For an unbaffled tank operating at 8 rpm, the residence time

in the sampling loop is 35 s but the residence time in the chamber is over 6 min. Therefore, it is important to improve O transfer in the chamber.

Baffles enhance O transfer by mixing the gas–liquid interface and increasing mass transfer, compared tó transport by passive diffusion. The baffles also work to move water with dissolved gas away from the surface, increasing the concentration gradient. As the baffles move from the liquid to the air, some water droplets remain on the baffle, further expediting O transfer. Figure 5 shows that the effect of the baffles is greater at higher rotation rates. The baffles do not transfer enough energy to the liquid at 2 rpm to result in a significant effect on O transfer.

The three-tube assembly, which passes through the center of the reactor, affects the axial mixing to some extent, if the liquid level in the reactor is high enough for the tubes to be in contact with the fluid. The lowest projecting tube just touches the liquid surface at a liquid volume of approx 1.5 L. For lesser volumes, dispersion occurs relatively slowly. A pulse of tracer might be visibly dispersed throughout the reactor within 2–3 time constants, with the time constant in this case defined as the sample loop flow rate divided by the overall liquid volume. If the liquid volume in the reactor is for example 2.0 L or greater, the tracer is dispersed more rapidly, since the periodic contact of the tube assembly with the liquid surface as the vessel rotates increases the speed and extent of axial mixing in the chamber.

Baffles improve axial liquid mixing by increasing bulk flow. Although the baffles are horizontal and rotate in the radial direction, the liquid is pushed toward the surface by wall baffles (pushed toward the wall by center baffles), and the momentum is carried axially after hitting the barrier (surface or wall). Examination of Fig. 8 shows a larger increase in D_e between one and two baffles than the increase between zero and one baffle or the increase between two and three baffles. With a single baffle in operation, the baffle is only submerged throughout half of each rotation. With two or more baffles in operation, there will always be at least one baffle submerged and, hence, the difference in D_e.

Modifying the location of the liquid inlet returning from the sampling loop further increases D_e. Instead of a single entry point at one end of the chamber, the liquid enters at multiple points, thereby effectively hastening the diffusion process.

ACKNOWLEDGMENTS

The authors would like to thank the US Bioreactor company for support of this project.

NOMENCLATURE

A Area at surface of well mixed entry region, cm^2

C_E Concentration in liquid at well mixed entry point of reactor, mol/L

C_{IN} Concentration in liquid entering reactor from sampling loop, mol/L
C_L Concentration in liquid, mol/L
C_{inf} Concentration at time = infinity
C_o Concentration at time = zero
D_e Axial dispersion coefficient, cm^2/s
F_F Volumetric flow rate through fresh feed spiroid, mL/s
F_S Volumetric flow rate through sampling spiroid, mL/s
k_La Volumetric gas–liquid mass transfer coefficient in reactor chamber, s^{-1}
k_La_{SL} Volumetric gas–liquid mass transfer coefficient in sampling loop, s^{-1}
L Reactor length, cm
t Time, s
t_R Residence time in sampling loop, s
u Velocity in sampling loop, flow rate divided by cross-sectional area, cm/s
V_L Liquid volume of reactor, mL^3
V_E Liquid volume at well-mixed entry point of reactor, mL^3
αC_G Dissolved oxygen concentration in liquid at saturation, mol/L
ϕ Dimensionless concentration, $C - C_{inf}/C_0 - C_{inf}$

REFERENCES

1. Abu-Reesh, I. and Kargi, F. (1989), *J. Biotechnol.* **9,** 167–178.
2. Petersen, J. F., McIntyre, L. V., and Papoutsakis, E. T. (1988), *J. Biotechnol.* **7,** 229–246.
3. Schurch, U., Karamer, H., Einsele, A., Widmere, F., and Eppenberger, H. M. (1988), *J. Biotechnol.* **7,** 179–184.
4. Phillips, K. L., Sallans, H. R., and J. F. T. Spencer (1961), *Ind. Eng. Chem.* **53,** 749–754.
5. Tanaka, H. (1982), *Biotechnol. Bioeng.* **24,** 425–442.